

Impacts of MgO waste:GGBS formulations on the performance of a stabilised natural high sulphate bearing soil

⁽¹⁾ *Adeleke, B.O., ⁽²⁾ Kinuthia, J.M., and ⁽³⁾ Oti, J.E.

⁽¹⁻³⁾ School of Engineering, Faculty of Computing, Engineering and Science, University of South Wales, Pontypridd, CF37 1DL, UK

*Corresponding author. Tel: +44 1443 482167, E-mail: blessing.adeleke@southwales.ac.uk

Abstract

Industrial and urban wastes have been generated overtime due to urban development with severe environmental and health implications. This paper reports the valorisation of waste and industrial by-product (magnesium oxide waste – MG1 and Ground Granulated Blastfurnace Slag – GGBS) to develop an alternative cementitious binder for suppressing swelling in high sulphate bearing soils, due to the formation of a highly expansive crystalline hydrate (ettringite) upon treatment with Portland Cement - PC or lime. Cylinder test specimens were developed using three MG1:GGBS proportions by weight (10:90, 20:80 and 30:70) to stabilise a natural Gypsum marl soil (GM) containing high levels of sulphate at varying stabiliser dosages (6, 8 and 10 wt.%), with PC as the control binder. UCS, Linear Expansion and SEM investigations were employed to assess the engineering suitability of the MG1:GGBS stabilised GM cylinder test specimen. Results suggest the viability of producing an alternative cementitious binder using up to 30 wt.% MgO-waste to successfully activate GGBS at stabiliser dosages of 6 - 10 wt.%. From a mechanical perspective, the MG1:GGBS stabilised GM soil was 1.5 – 3 times more than the control at 28 days moist curing age, while the resistance to linear expansion produced near zero swellings (0.13% – 0.2%) after 56 days, in comparison with the control of 3.2%. SEM micrographs showed a more compact structure with lesser voids and no morphology of ettringite. This new technology is expected to mitigate the environmental concerns of using PC and promote sustainable techniques of reusing industrial by-product materials for sulphate soils stabilisation.

Keywords: Sulphate bearing soil; Magnesium oxide waste; Soil stabilization; Mechanical strength; Linear expansion; Scanning electron microscopy; Ettringite.

1. INTRODUCTION

The choice of soil type on which various civil engineering structures are built is virtually impossible, whereby, requiring civil engineers to work with varied type of soils. However, with respect to civil engineering construction, some of the soil deposits in their natural form are suitable, others are suitable upon treatment (stabilisation), while some are unsuitable after treatment (problematic soil) due to their inherent composition that causes significant forms of swelling. Typical problematic soils are those containing certain levels of gypsum or calcium sulphates commonly known as sulphate-bearing soils (Kinuthia et al., 1999, Seco et al., 2011,

41 Seco et al., 2017, Diaz Caselles et al., 2020, Li et al., 2020). Pruška and Šedivý (2015) and
42 Dang et al. (2016) described the swelling phenomenon in soils as a three-dimensional problem,
43 which occurs when the fine particles of a soil material undergo a volumetric increase in size
44 due to the absorption of water from its surrounding as a result of the incessant changes or
45 fluctuation in moisture content caused by unstable seasonal weather conditions and flooding.
46 This volumetric increase in size is of key importance to the civil engineering industry due to
47 the generation of swelling and large magnitudes of swelling pressure, which leads to
48 destruction and additional refurbishment cost to structures (building foundations, rail tracks,
49 highway pavements, airports runways, tunnels, pipes, bridges, seaports etc) constructed in and
50 on the soil (Jones and Jefferson, 2012, Pruška and Šedivý, 2015).

51

52 Stabilisation of soils has been found to be economically and technically effective in reducing
53 swellings in expansive soils, by chemically altering the properties of the soil, which improves
54 the geotechnical and engineering properties of the stabilised/treated soil, using Portland cement
55 and Lime (Calcium based stabilisers) as activators, with various industrial by-products (Ground
56 Granulated Blast Slag - GGBS, Pulverised Fuel Ash - PFA, Silica Fume - SF, limestone dust
57 etc.) (Kinuthia and Oti, 2012, Miqueleiz et al., 2012, Phanikumar and Singla, 2016, Cheshomi
58 et al., 2017, Seco et al., 2017). Seco et al. (2011); Cheng and Heidari (2018) and Schanz et al.
59 (2018), all attributed this swelling tendency to the mineralogical composition/physiochemical
60 properties of the soil, type of clay with respect to Base Exchange Capacity (or cation exchange
61 capacity), quantity of clay, charge of exchangeable cations in the interlayer space, soil moisture
62 content, plasticity and dry density and the type of material used in case of soil stabilisation. A
63 number of studies have investigated and reported the reduction of this swelling tendency
64 through the application of calcium-based materials (Lime and PC) for stabilisation purposes
65 (Wang et al., 2003, Oti et al., 2009a, Oti et al., 2009b, Kinuthia and Oti, 2012). However,
66 researchers also highlighted that sulphate-bearing soils are prone to strength loss, stability and
67 durability risks due to the generation of expansive reactions, when treated or stabilised with
68 calcium-based stabilisers (Kinuthia et al., 1999, Kinuthia and Wild, 2001, Wang et al., 2003,
69 Rahmat and Kinuthia, 2011b, Nidzam and Kinuthia, 2010, Diaz Caselles et al., 2020). The
70 increased expansion was believed to be partly caused by the formation of a highly expansive
71 crystalline, and hydrated mineral from the hydration reaction of calcium (obtained from PC or
72 Lime), alumina, silica, sulphate in the presence of water known as ettringite
73 $[Ca_6Al_2(SO_4)_3(OH)_{12} \cdot 26H_2O]$ (Wild et al., 1999, Giliberto et al., 2008, Rahmat and Kinuthia,
74 2011a, Norman et al., 2013).

75

76 Apart from the negative impacts of calcium-based stabilisers (CBS) on sulphate bearing soils,
77 the deleterious effects of their production on the environment with respect to high energy
78 consumption (5240 MJ/ton for PC), increased emission of greenhouse gases and a large amount
79 of carbon dioxide (CO₂) footprint (0.66 – 0.9t CO₂ per tonne for PC) cannot be overemphasized
80 (Kinuthia and Wild, 2001, Juenger et al., 2011, Olivier et al., 2012, Behnood, 2018, Wang et
81 al., 2019, Olivier and Peters, 2019). Furthermore, there is a current substantial growth in the
82 amount of stored or landfilled wastes, which had considerably grown over the past years due
83 to the reliance of the global economy on the development of materials (e.g. PC) with
84 exhaustible natural resources (Górák et al., 2020). Taking the construction industry as a case
85 study, there is a significant consumption of about 40 – 75% natural (virgin) materials, coupled
86 with the generation of proportionate wastes during its extraction, and all through the stages of
87 manufacture of the finished product; thus, the demand for the natural materials is growing and
88 growing each year (John et al., 2011, El-Dieb and Kanaan, 2018, Górák et al., 2020). Therefore,
89 current industrial organizations should endeavor to achieve sustainability through the effective

90 management of generated wastes (Gopinath et al., 2018). Goals nine and eleven of the United
91 Nations sustainable development goals aimed at “*building resilient infrastructure, promote*
92 *inclusive and sustainable industrialization and foster innovation*” and to “*make cities and*
93 *human settlements inclusive, safe, resilient and sustainable*” (United-Nations, 2015). Based on
94 this understanding, we are now faced with a situation where the global construction industry is
95 rediscovering large-scale interest in materials that, for decades, held largely niche or curiosity
96 value (e.g. magnesium oxide - MgO) leading to an ongoing search for alternatives to PC
97 (Juenger et al., 2011, Juenger and Siddique, 2015).

98
99 Recently, magnesium oxide (MgO) cementitious systems have been investigated by various
100 researchers to mitigate the negative environmental impacts of PC, by employing it as an
101 activator within a cementitious binder system (Jin et al., 2015, Yi et al., 2016, Wang et al.,
102 2016), and demonstrated positive potentials to performing the expected functions of an
103 activator within cementitious binder systems. Yi et al. (2015b) compared the use of MgO and
104 PC for developing cementitious binder systems and found a 70 - 72% less energy consumption,
105 65 - 79% CO₂ emission reduction and 6 - 13% reduction in the cost of MgO production
106 compared to PC. Generally, the principal cementitious hydrate from the hydration reaction of
107 CBS (e.g PC) is the Calcium Silicate Hydrate gel (C-S-H). Hence, a cementitious binder system
108 that is based on MgO as the primary alkaline activator results in the formation of a Magnesium
109 Silicate Hydrate gel (M-S-H) gel that is similar to the C-S-H gel (Wu et al., 2018). The
110 formation of the nanosized phyllosilicates gel cementitious hydrate (M-S-H gel) using MgO
111 demonstrated its potentials within a MgO-SiO₂-H₂O system using cement pastes (Li et al.,
112 2014, Roosz et al., 2015, Bernard et al., 2019). MgO is produced majorly from Magnesite
113 (MgCO₃), which is the magnesium end member of an isomorphous series of carbonates occurs
114 naturally as a sedimentary rock (Jin and Al-Tabbaa, 2014). Magnesite mines remains the major
115 source of raw material for the production of MgO, amounting to about 20 million tonnes per
116 year (80% of which is produced in China) and other sources for MgO production are from
117 brines and seawater (Gu et al., 2014). This claim was also corroborated by the United States
118 geological survey, which estimated a total production of 6970 metric tonnes of magnesite in
119 the world with China coming tops with a production of 4900 metric tonnes and Spain (the only
120 European country with magnesite deposits) with a production of 280 metric tonnes (USGS,
121 2020). Therefore, the large production of magnesite with the sole aim of producing MgO
122 provides a basis for the expected production and availability of MgO wastes.

123
124 MgO can be considered a more environmentally friendly stabiliser additive to PC because of
125 its lower manufacturing impact/cost (Ruan and Unluer, 2016). Yi et al. (2014) demonstrated
126 that after 28 days of moist curing, an appropriate proportion of MgO and GGBS enhanced the
127 mechanical strength properties of a stabilised soil in comparison with PC. Several researchers
128 corroborated this claim by suggesting that the enhancement of the physical and mechanical
129 properties of a natural soil is due to the formation of the C-S-H gel and M-S-H gel (Jin et al.,
130 2015, Yi et al., 2016, Goodarzi and Movahedrad, 2017). The reactivity and economic suitability
131 of low-grade magnesium oxides obtained as by-products in the calcined magnesite
132 manufacturing was demonstrated by del Valle-Zermeño et al. (2015) for environmental
133 applications in remediation and/or wastewater treatment. Seco et al. (2017) also observed that
134 magnesium-based additive enhanced the engineering properties of sulphate soils better than
135 calcium-based ones. In that investigation, five sulphate soils with no clear sulphate content
136 reached unconfined compressive strength above 10 MPa after 21 days, surpassing the
137 requirements of a subbase layer (Ardah et al., 2017). Another beneficial effect of the
138 magnesium stabilisation was the decrease of the soils’ swell strain after prolonged exposure to

139 moisture. Li et al. (2020) demonstrated the advantage of a MgO-GGBS binder in a sulphate
140 soil against swelling and better mechanical strength gain after test samples were soaked when
141 compared to PC. These results suggest the potential of stabilisation of local sulphate soils with
142 Mg based binders. Currently, experimental studies on soils stabilisation using MgO based
143 binders are mainly focused on natural soils, with the suggestion of using about 10 - 20%
144 stabiliser dosage (Gu et al., 2014, Yi et al., 2015a, Yi et al., 2016). In addition, recent
145 investigations on sulphate soil stabilisation using MgO suggested a 4% stabiliser dosage for a
146 natural sulphate-bearing soil with no clear indication of its sulphate content (Seco et al., 2017),
147 while Li et al. (2020) also suggested a 10% stabiliser dosage for an artificially induced sulphate
148 bearing Kaolinite clay with a 3.6wt.% bassanite (gypsum) content (2wt.% sulphate).

149
150 Due to the lack/insufficient amount of knowledge on the appropriate MgO based stabiliser
151 dosage for stabilising natural high sulphate soils, possibility of developing cementitious binder
152 systems using MgO waste as an activator as opposed to previous studies that employed the use
153 of commercial MgO binders and experimental simulation of a sulphate soil system, and
154 potential application of the developed cementitious binder to reduce swelling in natural high
155 sulphate soil using the technique of chemical stabilisation, this paper presents an evaluation of
156 the engineering performance and microstructural properties of a stabilised natural high sulphate
157 soil using MgO-waste activated GGBS binder. It is expected that the use of reactive MgO
158 wastes could become an additional environmental advantage by reducing the manufacturing or
159 reliance on commercial MgO products (which could be expensive) rather than utilising its
160 waste streams that was obtained during the manufacturing process. In addition, there will be a
161 reduction in the production of CBS that are deleterious to the environment with respect to high
162 energy consumption, increased emission of greenhouse gases, large amount of CO₂ footprint
163 (Juenger et al., 2011, Olivier et al., 2012) and the potential reduction of swelling in high
164 sulphate-bearing soils (Kinuthia and Wild, 2001, Seco et al., 2017, Behnood, 2018).

165

166 **2. METHODOLOGY**

167 2.1 Materials

168 The materials used in this study were Gypsum marl clay (GM), Portland cement - PC (CEM I-
169 42.5N), Magnesium oxide waste (MG1), Ground Granulated Blast-furnace Slag (GGBS) and
170 De-ionized water. GM was a natural soil with approximately 22 wt.% sulphate (SO₃) content
171 that was obtained from the Ebro's Valley in Navarra, Northern Spain. PC was manufactured in
172 compliance with BS EN 197-1:2011 and supplied by Lafarge Cement UK, while GGBS as a
173 latent hydraulic material was supplied and used in accordance with BS EN 15167-1:2006 by
174 Civil and Marine Ltd, Llanwern, Newport, UK. MG1 is a waste product obtained as a by-
175 product during the mining activities of magnesite (MgCO₃) by Magnesitas Navarras, Navarra,
176 Spain. Table 1 shows the corresponding chemical compositions and other relevant properties
177 for the raw materials. The chemical compositions were obtained using a portable benchtop
178 TXRF X-ray Fluorescence spectrometer, which is comprised of an air-cooled low power X-ray
179 metal-ceramic tube with a molybdenum target. It runs at a max power of 50 W with a liquid
180 nitrogen-free Silicon Drift Detector (SSD)(BS EN 15309:2007, BS ISO 18227:2014).

181

182

183

184

185

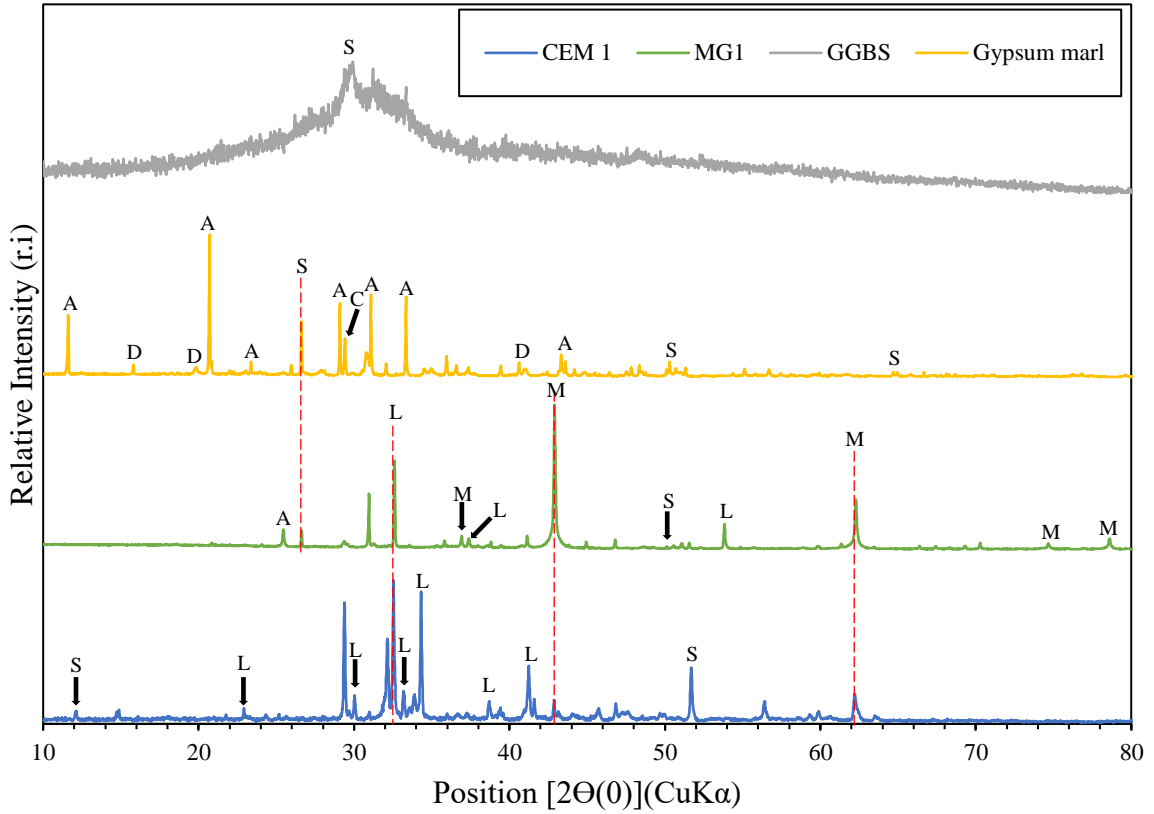
Table 1: Chemical composition of Kaolinite clay, CEM I and GP

Oxides	Composition (wt%)			
	CEM I	MG1	GGBS	Gypsum marl
CaO	61.49	9.39	37.99	23.16
SiO ₂	18.84	2.51	35.54	16.97
Al ₂ O ₃	4.77	0.52	11.46	6.70
MgO	3.54	56.26	8.78	3.21
Fe ₂ O ₃	2.87	2.13	0.42	2.03
Mn ₂ O ₃	0.05	0.15	0.43	0.04
SO ₃	3.12	6.22	1.54	22.39
TiO ₂	0.26	0.01	0.70	0.21
K ₂ O	0.57	0.18	0.43	1.39
Na ₂ O	0.02	0.09	0.37	0.77
P ₂ O ₅	0.10	0.06	0.02	0.07
V ₂ O ₅	0.06	0.10	0.04	0.02
BaO	0.05	0.01	0.09	0.02
L.O.I.	4.30	22.30	2.00	23.00
Physical Properties				
Colour	Grey	Light-Brown	Off-white	Grey
Specific gravity	3.16	2.86	2.90	2.33
Reactivity (m)	-	30	-	-

187

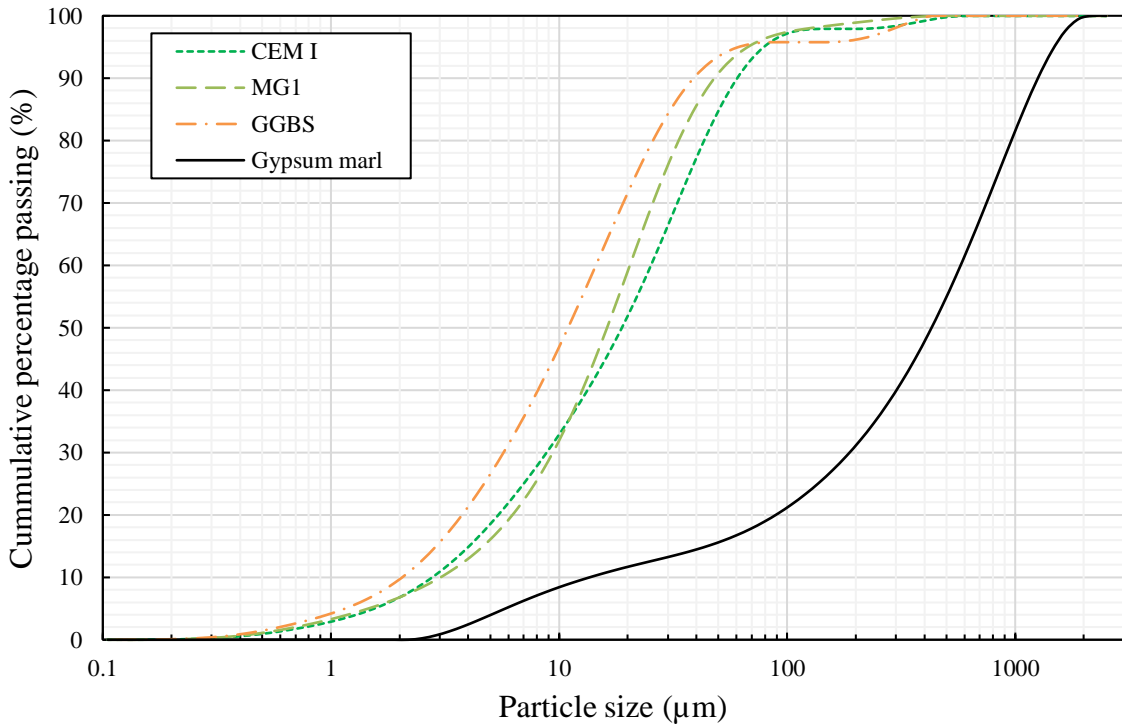
188

189 The X – ray diffractograms in Figure 1 showed the crystallized forms for the primary materials
 190 (CEM I, MG1, GGBS and GM) used in this study as periclase, lime, quartz, gypsum
 191 (anhydrite), dolomite and calcite. However, observation showed a glassy phase for GGBS. The
 192 particle distribution curves for the raw materials are shown in Figure 2 and indicates a rather
 193 higher proportions of fine particles for MG1 in relation to CEM I. The reactivity of MG1 was
 194 carried as described by Shand (2006) to determine the rate of acid neutralization and
 195 established as a reactive MgO.



196 Periclase (MgO) - M, Lime (CaO) - L, Quartz (SiO₂) - S, Gypsum (Anhydrite - CaSO₄) - A,
 197 Dolomite (CaMg(O₆)₂) - D, Calcite (CaCO₃) - C
 198

199 **Figure 1:** X-ray diffractograms for the materials
 200
 201



202 **Figure 2:** Particle size distribution curves for the raw materials
 203

204 **2.2 Mix design, test sample preparation and experimental testing**

205 Tables 2 shows the mix compositions that were developed and used in this study to produce
 206 cylindrical test specimens. In accordance with the findings of Adeleke et al. (2020), an 8 wt.%
 207 optimum stabilizer dosage using CEM I for a simulated high sulphate bearing soil was used as
 208 the control for the current study. The MG1:GGBS binder compositions were developed at three
 209 MG1:GGBS proportions by weight of 10 : 90, 20 : 80 and 30 : 70 to stabilise GM at varying
 210 stabiliser dosages of 6, 8 and 10 wt.%. The MG1 content within the MG1:GGBS binder
 211 compositions corresponds to 10, 20 and 30wt.%. It is imperative to note that the mix code of
 212 1M, 2M and 3M which denotes 10wt.%, 20wt.% and 30wt.% of MG1, while 7G, 8G and 9G
 213 which denotes 70wt.%, 80wt.% and 90wt.% of GGBS will be used all throughout this study.

214

215

Table 2: Mix design using Gypsum marl soil

Mix code	Stabiliser dosage (wt.%)	Mix composition	Binders (g)			Target Material (g)	Water (g)	Total weight (g)
			M	G	CEM I	GM		
BG1a	8	8CEM I - GM	-	-	26.2	374.4	51.9	452.5
BG6-1	6	1M:9G - GM	2.3	20.4	-	377.9	47.6	448.2
BG6-2		2M:8G - GM	4.5	18.1	-	377.9	47.6	448.2
BG6-3		3M:7G - GM	6.8	15.9	-	377.9	47.6	448.2
BG8-1	8	1M:9G - GM	3.0	26.7	-	370.9	47.6	448.2
BG8-2		2M:8G - GM	5.9	23.7	-	370.9	47.6	448.2
BG8-3		3M:7G - GM	8.9	20.8	-	370.9	47.6	448.2
BG10-1	10	1M:9G - GM	3.6	32.8	-	364.2	47.6	448.2
BG10-2		2M:8G - GM	7.3	29.1	-	364.2	47.6	448.2
BG10-3		3M:7G - GM	10.9	25.5	-	364.2	47.6	448.2

M – MG1; CEM I - Portland cement; G - Ground Granulated Blastfurnace slag; GM - Gypsum marl soil

216

217 Dry materials capable of producing three compacted cylindrical test specimens from each
 218 binder composition, each of dimensions 50 mm in diameter and 100 mm in length, were
 219 thoroughly mixed in a mechanical mixer for 2 minutes before slowly introducing the
 220 predetermined amount of water. Intermittent hand mixing with a palette knife was
 221 accomplished for another 2 minutes to achieve a homogeneous mix, and to ensure that the full
 222 potential of stabilisation was achieved. Each compacted cylindrical test specimen was made by
 223 placing the wet material of each sample in a steel mould fitted with a collar (Figure 3), so as to
 224 accommodate all the materials. This material was then subjected to a static compression using
 225 a hydraulic jack to achieve the desired maximum dry density (MDD) in a loading frame, while
 226 the volume was kept constant. Afterwards, the cylindrical test specimen was wiped of any

227 clinging soil particles or oil stains, weighed, labelled, and wrapped with a cling film to ensure
228 minimal loss of moisture. Thereafter, the specimens were placed in a sealed plastic box, stored
229 for moist curing at a temperature of $20 \pm 2^{\circ}\text{C}$ for a duration of 7, 28 and 56 days prior to testing.
230 The plastic container helped in the regulation of the humidity at which they are cured, and
231 prevent any deleterious carbonation effect which is common to stabilised soil systems.

232 The mechanical performance of the cylindrical test specimen was investigated using the
233 Unconfined Compression Strength (UCS) test in compliance with BS 1924 - 2:2018, using an
234 Instron 8502 mechanical testing machine, which is capable of loading over 10kN (Figure 4).
235 Three test samples per mix composition were tested for compressive strength at the end of the
236 moist curing period of 7, 28 and 56 days until failure occurs at a compression strain rate of 1
237 mm/minute. The maximum load at the point of failure for each cylindrical test specimen was
238 recorded and the mean of three strength values are used as the representative UCS value for
239 the mix composition. The swelling/shrinkage performance (%) of the cylindrical test specimen
240 was achieved by utilising a Linear expansion test. This was carried out in accordance with BS
241 EN 13286-49:2004 by measuring the amount of expansion using a Perspex cell, which was
242 equipped with a digital dial gauge (Figure 5). The linear expansion measurements were
243 monitored and recorded during the moist curing and partial soaking period in water for every
244 24 hours, until no further significant swelling was detected.

245

246

247

248

249

250

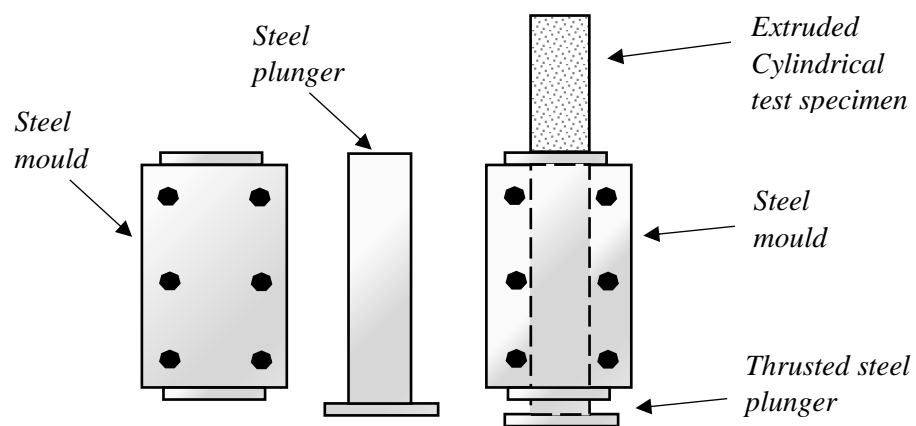
251

252

253

254

255



256

Figure 3: Steel mould with the extruded cylindrical test specimen



*Tested
cylindrical
specimen*

257

258

Figure 4: An Instron 8502 mechanical testing machine

259

260

261

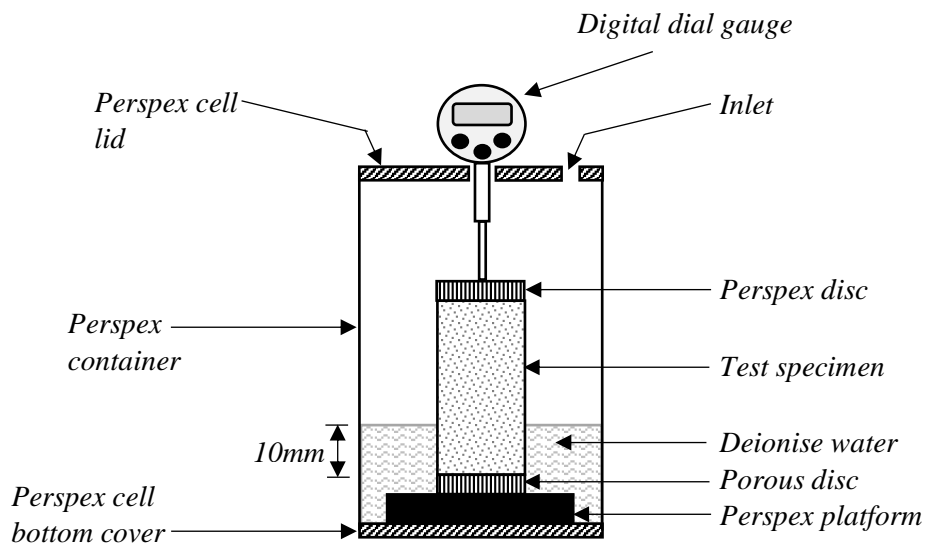
262

263

264

265

266



267

Figure 5: Schematic diagram of a Perspex cell test set-up

268

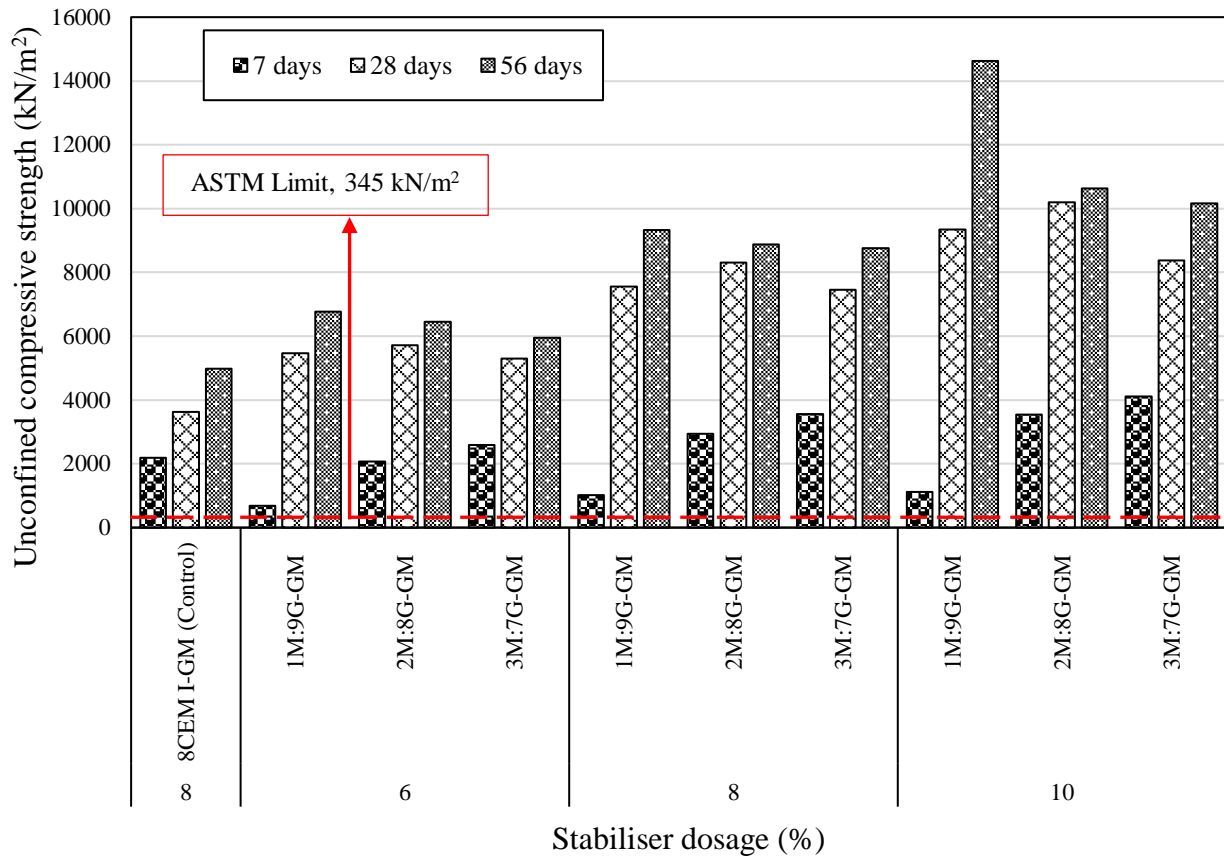
269 A microstructural investigation was employed to analyse the morphology of each hydrated
 270 dried specimen using a MIRA3 TESCAN Scanning Electron Microscope (SEM), which was
 271 fitted with a Solid-state Backscattered (electron) Detector (SBD). Initial sample preparation
 272 was carried out by placing the cylindrical test specimen in a desiccator cabinet, and at a low
 273 temperature of 40⁰C containing silica gel for accelerated drying of the specimen. Thereafter, a
 274 diamond wheel tile cutter was used to produce small slices (5mm thickness) of the dried
 275 cylindrical specimen. Each slice from the sample was initially polished, gold coated and
 276 infused on a stub made up of carbon tapings to make the specimen electrically conductive.
 277 Afterwards, the stub was mounted on the sample stand in the SEM chamber before the
 278 commencement of the SEM analysis.

280 3. RESULTS

281 3.1 *Unconfined Compressive Strength (UCS) test*

282 Figure 6 presents the Unconfined Compressive Strength (UCS) results of GM cylinder test
283 specimens (10wt.% MG1:90wt.% GGBS – 1M:9G; 20wt.% MG1:80wt.% GGBS – 2M:8G;
284 30wt.% MG1:70wt.% GGBS – 3M:7G proportions), which were stabilised with 6, 8 and 10
285 wt.% of MG1:GGBS binder compositions at both 7, 28 and 56 days moist curing periods. A
286 steady increase in strength development was observed for all the GM cylinder test specimens
287 in all cases of stabiliser dosages (6, 8 and 10 wt.%) at every moist curing age of 7, 28 and 56
288 days. However, an average rate of strength development was more pronounced at the 28 days
289 moist curing age in comparison with 7 and 56 days for all the binder compositions at varying
290 stabiliser dosages (6 – 10wt.%).

291 At 7 days moist curing age, a gradual trend of strength increase was experienced by all the GM
292 cylinder test specimens with increasing MG1 content within the varying MG1:GGBS binder
293 compositions (1M:9G; 2M:8G and 3M:7G) for all stabiliser dosages (6 – 10 wt.%). This trend
294 was not the case for other moist curing ages as there was a staggered strength development for
295 the binder compositions at 28 days, with blend composition 2M:8G attaining the highest UCS
296 strength across the stabiliser dosages. However, a reduction or slow increase in UCS was
297 observed at 56 days moist curing for every increase in MG1 content within the MG1:GGBS
298 binder compositions at all stabiliser dosages (6 – 10 wt.%). The lowest magnitude of UCS
299 value was produced by the control mix cylinder test specimen composed of 8wt.% CEM I at
300 28 days moist curing age at all cases of stabiliser dosage (6, 8 and 10 wt.%), while the largest
301 strength magnitude was experienced by cylinder specimens stabilised with 20wt.%
302 MG1:80wt.% GGBS composition. At later moist curing age (56 days), this trend changed in
303 favour of the cylinder test specimens stabilised with 10wt.% MG1:90wt.% GGBS composition
304 to achieve the maximum UCS value of 6769, 9320 and 14626 kN/m² at 6, 8 and 10wt.%
305 stabiliser dosages, respectively. An average strength increase was observed within the range of
306 11 – 48%, 20 – 45% and 12 – 47% at every increase in stabiliser dosage (6, 8 and 10wt.%) for
307 all the GM cylinder test specimens stabilised with 1M:9G, 2M:8G and 3M:7G binder
308 compositions respectively.



310

311 **Figure 6:** Combined UCS test results at 7, 28 and 56 days curing age for GM cylinder test specimens
 312 stabilised with varying stabiliser dosages (6, 8 & 10 wt.%) of MgO-waste activated GGBS binder
 313 compositions
 314

315 Generally, all the cylinder specimens that were produced using the MG1:GGBS binder
 316 compositions (1M:9G; 2M:8G and 3M:7G) produced superior strength performances at all the
 317 investigated stabiliser dosages in comparison with the control cylinder specimen, at the
 318 standardised curing age of 28 days.

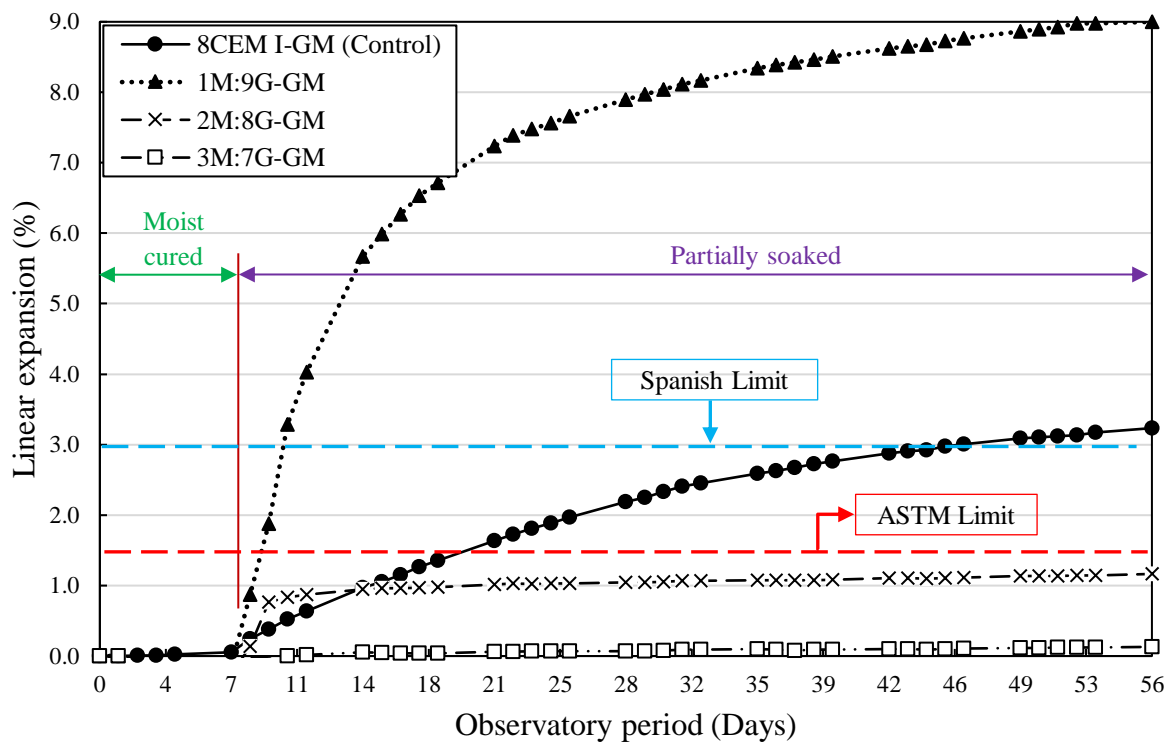
319

320 3.2 Linear expansion test

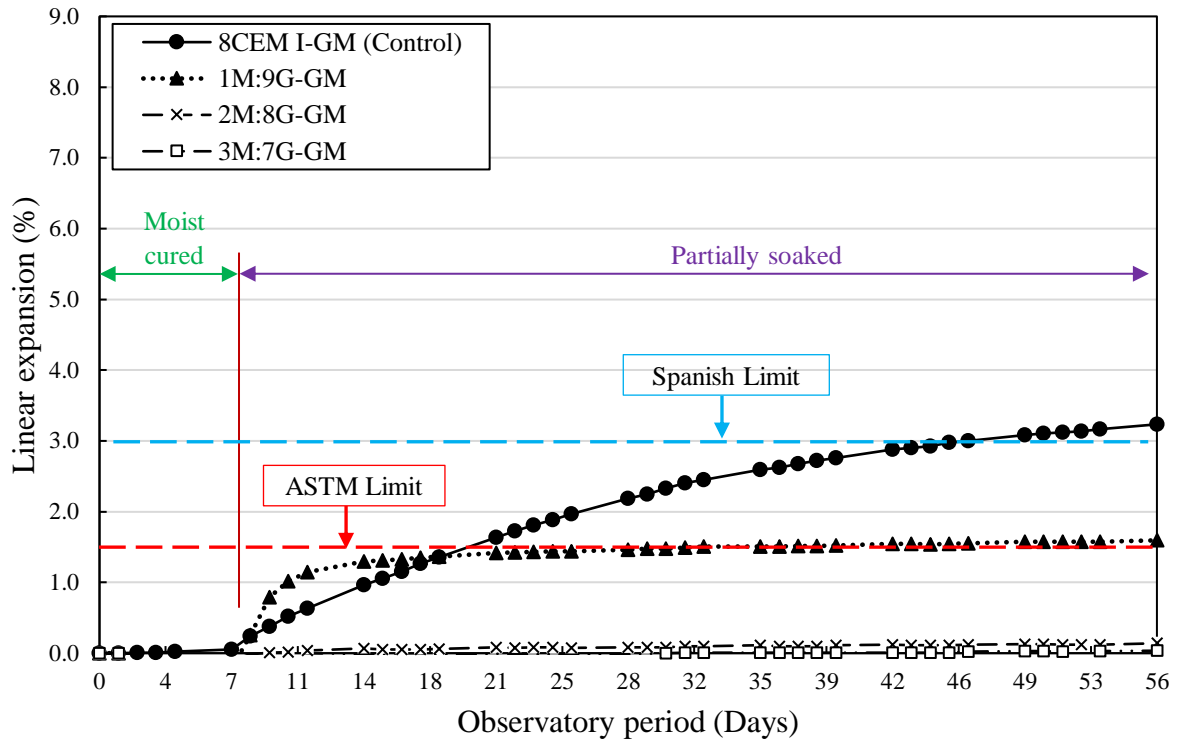
321 The typical linear expansion plots for GM cylinder test specimens, that were stabilised with 6,
 322 8 and 10 wt.% of MG1:GGBS binder contents during a moist curing and subsequent partial
 323 soaking conditions is shown in Figure 7 – 9.

324 A marginal increase in linear expansion can be seen for the GM cylinder test specimens
 325 produced for the three MG1:GGBS binder contents (6, 8 and 10 wt.%) after 7 days of moist
 326 curing. A maximum linear expansion of 9% was experienced by cylinder specimens stabilised
 327 with 6 wt.% of 10wt.% MG1:90wt.% GGBS blend composition, while the control cylinder
 328 specimen with 8 wt.% CEM I experienced a maximum expansion of 3.2% at both 8 and 10
 329 wt.% binder dosage. It was also observed that there was a reduction in linear expansion for
 330 every increase in the MG1 waste content within the MG1:GGBS blend compositions. This
 331 observation suggests why the lowest linear expansion of 0.13, 0.04 and 0.20% were detected
 332 for the GM cylinder test specimens containing 30wt.% MG1:70wt.% GGBS blend composition
 333 at 6, 8 and 10 wt.% binder dosage after 49 days of partial soaking in deionised water.

334 Furthermore, a reduction in the linear expansion was evident in the GM cylinder test specimens
 335 containing 10wt.% MG1:90wt.% GGBS and 20wt.% MG1:80wt.% GGBS blend composition
 336 with every increase in the amount of binder dosage. However, this was not the case for cylinder
 337 test specimens with 30wt.% MG1:70wt.% GGBS blend composition, as they already exhibited
 338 stability in linear expansion using a range of 6 – 8wt.% stabiliser dosage. A trend of potential
 339 propagation of further linear expansion at increased stabiliser content for cylinder specimen
 340 with increased level of MG1 content is evident in Figure 9. This suggests that stabiliser dosages
 341 above 10 wt.% could result in the propagation of further linear expansion. Observation also
 342 showed that the GM cylinder test specimens that were produced using the control blend mix (8
 343 wt.% CEM I) and 10wt.% MG1:90wt.% GGBS blend at 6 wt.% binder content, exceeded both
 344 expansion benchmarks as established in the American standard of measurement (ASTM) –
 345 1.5% (ASTM D4829 - 11) and the legal limit of 3% in Spain as reported by Seco et al.
 346 (2011).for stabilised soil systems. Furthermore, the GM cylinder test specimen with 10wt.%
 347 MG1:90wt.% GGBS blend slightly went over the ASTM limit (1.5%) at an increased binder
 348 dosage of 8 wt.%, after 17 days of been partially soaked in deionised water.
 349
 350

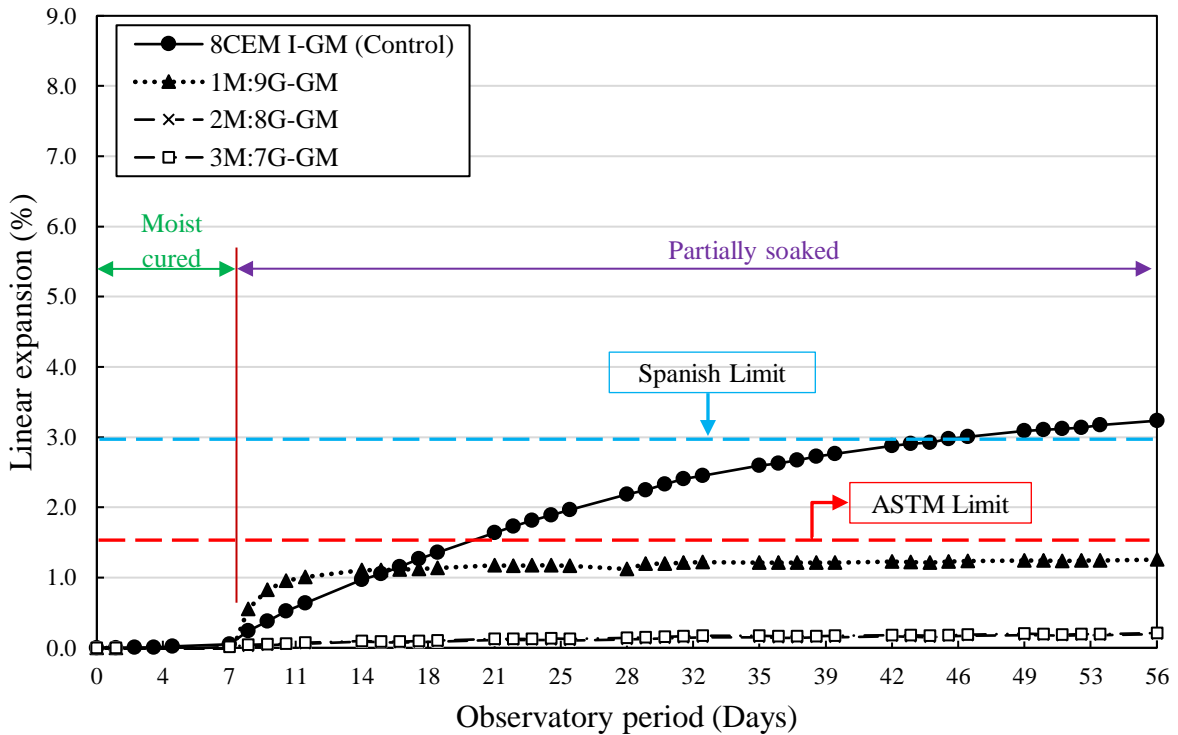


351
 352 **Figure 7:** Typical plots of linear expansion against observatory period for GM cylinder test
 353 specimens containing varying levels of MG1:GGBS content and stabilised with **6 wt.%** binder dosage
 354 at both moist and partially soaked curing conditions
 355
 356
 357



358
359
360
361

Figure 8: Typical plots of linear expansion against observatory period for GM cylinder test specimens containing varying levels of MG1:GGBS content and stabilised with **8 wt.%** binder dosage at both moist and partially soaked curing conditions



362
363
364
365
366

Figure 9: Typical plots of linear expansion against observatory period for GM cylinder test specimens containing varying levels of MG1:GGBS content and stabilised with **10 wt.%** binder dosage at both moist and partially soaked curing conditions

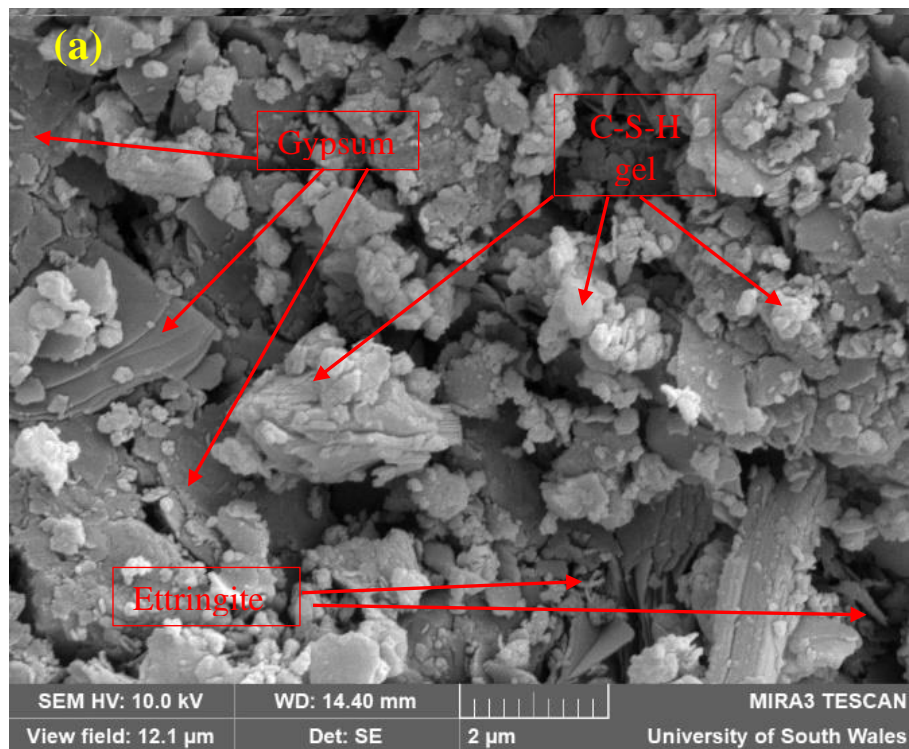
367 **3.3 Microstructural investigation**

368 Figures 10 and 11 present the SEM micrographs from the fragments obtained from stabilised
369 samples of GM cylinder test specimen using 8wt.% CEM I (Control) and 6 wt.% binder dosage
370 of 30wt.% MG1:70wt.% GGBS composition (3M:7G), at 28days for different curing
371 conditions (moist curing and partial soaked).

372 It was observed that the morphology of the stabilised GM using 8wt.% CEM I (Control) in
373 Figure 10(a) is very different to that of the MG1-activated GGBS binders in Figure 10(b),
374 which confirms the formation of a different type of microstructure after 28 days of moist curing
375 condition. This trend was also similar to the SEM images that were obtained in Figure 11 for
376 both stabilised Gypsum marl soil using CEM I and MG1-activated GGBS binders after 28 days
377 of partial soaking in deionised water.

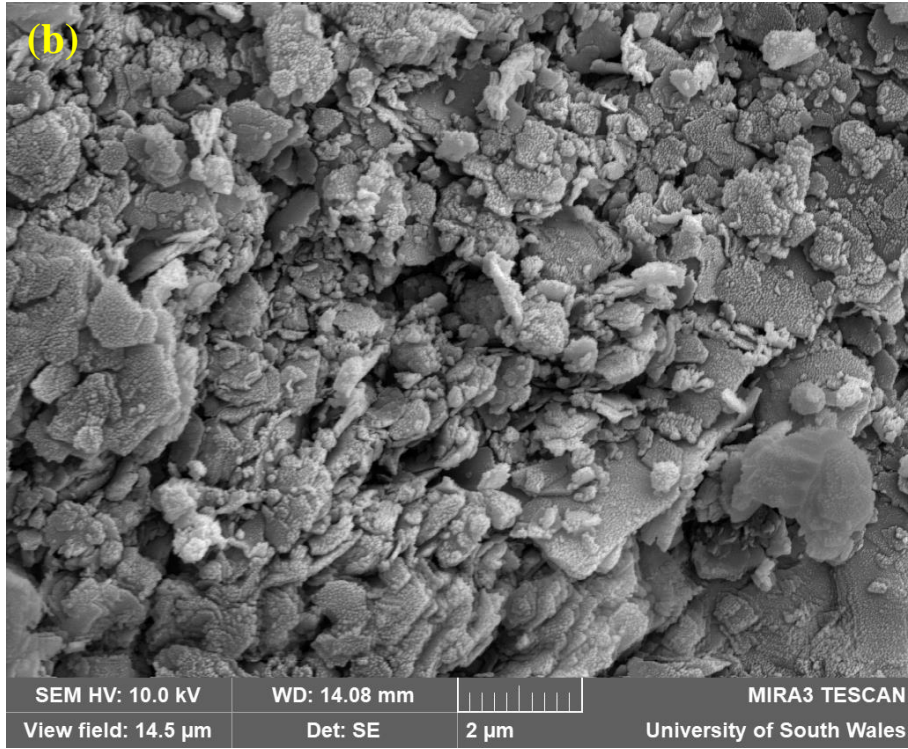
378 It was also seen from the SEM micrographs in Figure 10 that the Control GM stabilised sample
379 under moist curing condition produced a hydration compound which consists of small globular-
380 like particles clumped together with no definite shape known as C-S-H gel. Additionally, flat
381 sheets of gypsum (sulphate) and ettringite crystal precipitates were also visually identified as
382 some of the hydration compounds (Li et al., 2020, Diaz Caselles et al., 2020). However, a visual
383 inspection of the GM samples that were stabilised with 6wt.% MG1-activated GGBS binder
384 showed a relatively flocculated structure of the soil particles. The SEM micrographs in Figure
385 11(a) shows the formation of large quantities of ettringite structures, hydration compound (C-
386 S-H gel) and gypsum in the GM soil that was stabilised with CEM I after partial soaking
387 conditions for 28 days. However, Figure 11(b) still showed a more compact structure with
388 almost little voids even after partial soaking for 28 days.

389



390

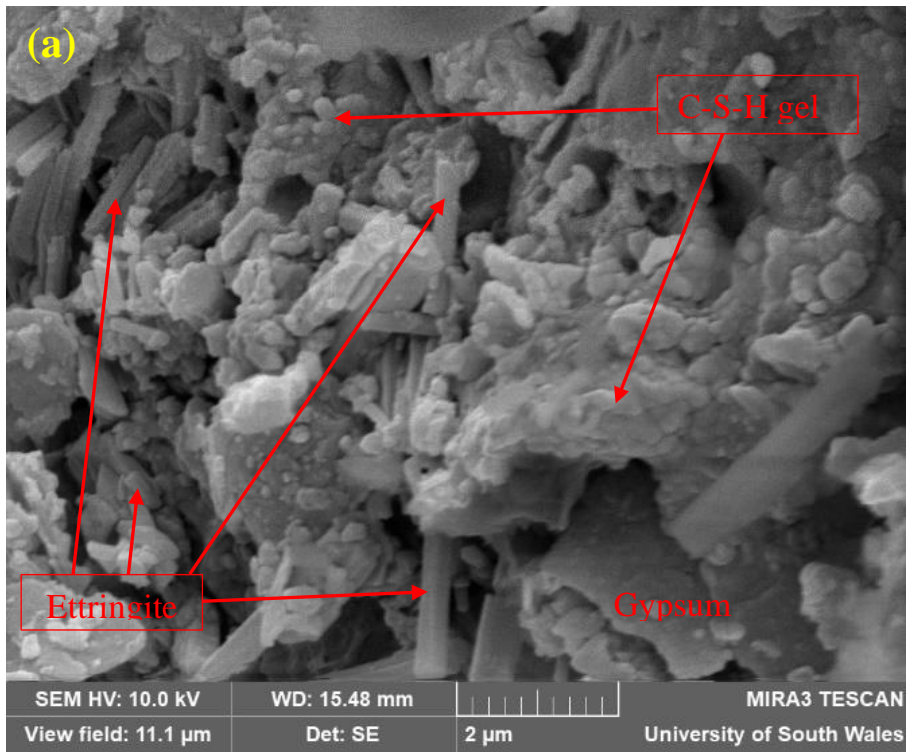
391



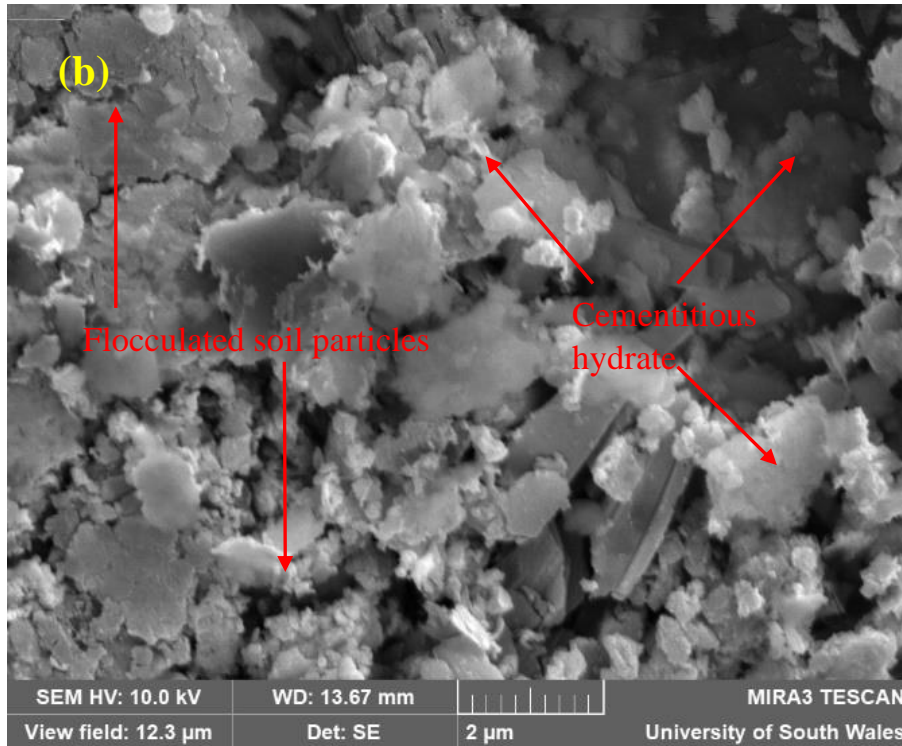
392

393 **Figure 10: SEM micrographs of stabilised Gypsum marl soil after 28 days moist curing condition**
 394 using (a) 8 wt.% CEM I binder dosage at 2µm resolution, and (b) 6 wt.% binder dosage of 3M:7G
 395 composition at 20µm resolution.

396



397



398

399

400

401

402

403

404 4. DISCUSSIONS

405 4.1 Mechanical performance of stabilised GM soil with MgO-waste binders

406

407

408

409

410

411

412

413

414

415

416

417

418

419

420

421

422

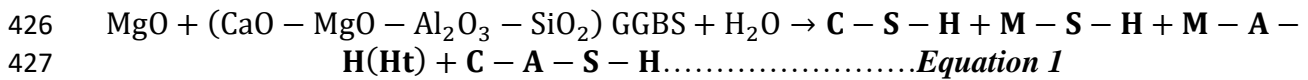
423

424

Figure 11: SEM micrographs of stabilised Gypsum marl soil after **28 days partially soaking condition** using (a) **8 wt.% CEM I binder dosage at 2μm resolution**, and (b) **6 wt.% binder dosage of 3M:7G composition at 2μm resolution**.

An effective stabilisation effort on soils requires that a certain UCS value is achieved at either 7 or 28 days of moist curing age, as it will be a direct indicator of the efficacy of the MgO-waste's potential at activating GGBS. The display of strength gain by all the stabilised GM cylinder test specimens in all cases of stabiliser dosage (6, 8 and 10 wt.%) could be attributed to the hydration reaction caused by the successful activation of GGBS by MG1 (MgO waste material) over the curing period. Goodarzi and Movahedrad (2017) corroborated this claim and suggested that the gain in strength could as well be the formation of more cementing hydrate/phases which fills up the colloidal spaces, and subsequently lead to interlocking of the clay particles. The main cementing hydrate/phases that are formed during a pozzolanic reaction (hydration) within the stabilised cylinder specimen using the MG1:GGBS blend composition are Magnesium Silicate Hydrate (M-S-H gel) or Hydrotalcite – Ht (Zhang et al., 2014, Yi et al., 2015b, Abdalqader et al., 2015, Li et al., 2020). The activation process of GGBS by MG1 begins with an initial destruction of the bonds within the GGBS composition e.g., Mg – O, Ca – O, Si – O – Si, Al – O – Si and Al – O – Al, which is subsequently followed by the development of a Si – Al inter-surface layer over the grains of the GGBS material. Thereafter, Mg²⁺ either reacts with Si–O or Al–O to produce a cementing hydrate mainly as C-S-H gel and M-S-H gel or Hydrotalcite/Magnesium Aluminate Hydrate – M-A-H (Darko and Branislav, 2002, Jin et al., 2015). Therefore, an overall hydration reaction for the MG1:GGBS binder composition can be summarized in Equation 1.

425



428

429 The formation of C-S-H and C-A-S-H within the stabilised system using MG1:GGBS binder
 430 composition is as a result of the available Ca content within the elemental composition of each
 431 material (MG1 and GGBS). However, this is not of major concern as the hydration products
 432 are of very minute quantity with no substantial negative impact on the UCS of the stabilised
 433 system during the moist curing period. It is also important to note that the presence of brucite
 434 ($Mg(OH)_2$) within the first stage of hydration could be deleterious to the overall stabilised
 435 matrix, if there are not enough hydration conditions (adequate alkalinity level, water content
 436 and temperature) for complete dissolution of brucite to form the cementitious M-S-H gel (Jin
 437 and Al-Tabbaa, 2013, Gomes and de Oliveira, 2018). Another obvious justification for the
 438 increase in UCS performances at 28 days curing age, could be due to the increase in curing age
 439 for each mix compositions that allows for the production of more cementing gel (M-S-H) as a
 440 result of the pozzolanic reaction.

441

442 The initial slow development of UCS strength that was observed for the MG1:GGBS binder
 443 with 10 wt.% MG1 in the stabilised GM cylinder specimens in comparison with the control at
 444 7 days, could be ascribed to the higher reactivity of Ca during the initial stage of hydration,
 445 which produces faster cementing gels (only C-S-H) necessary for strength gain. However, this
 446 was not the case at 28 days as the pozzolanic reaction set in to form different types of cementing
 447 hydrates (some amount of C-S-H but more of M-S-H gels) necessary for further strength gain.
 448 This finding agrees with that of Wang et al. (2016) and Goodarzi and Movahedrad (2017), who
 449 also suggested that the M-S-H gel or Ht compounds are very large compared with C-S-H and
 450 can increase the level of long-range structural efficiency of the hydration elements, which
 451 provides the necessary binding capacity that will lead to greater strength in the stabilised soil.
 452 It is worthy to note that the presence of sulphate within the GM soil system did not pose any
 453 reduction to UCS of the stabilised cylinder specimens. This observation could be credited to
 454 the reduced presence of available Ca within the stabilised system that would have reacted with
 455 the available sulphate to form the needle-like ettringite crystals that could have been
 456 detrimental to the overall stabilised system. Hence, the sulphate content was coated with the
 457 cementing gel that was produced, remained dormant within the stabilised system, and could
 458 have contributed to the overall compressive strength of the stabilised cylinder specimen due to
 459 its crystalline nature. The UCS performance also showed that high MG1 contents within the
 460 range of 20 to 30wt.% of the MG1:GGBS composition can accelerate the strength development
 461 of GGBS stabilised sulphate soils at 7 and 28 days moist curing age. However, some reduction
 462 and slow increase in strength gain was observed at 56 days curing. This showed that high
 463 amounts of MG1 content can act as a negative impact on the UCS performance at later stages.
 464 Yi et al. (2016) also attributed this reduction in UCS performance to the type of MgO (reactive)
 465 that was used within the MG1:GGBS composition. Therefore, lower amounts of reactive MG1
 466 contents (10 wt.%) with large GGBS content (90 wt.%) is suggested for a continuous
 467 pozzolanic activity, as it will result in further strength development within the investigated
 468 sulphate stabilised system. In addition, the application of an acceptable UCS threshold of 345
 469 kN/m^2 for stabilised products using waste materials was established, as all the investigated mix
 470 combinations are in compliance with the ASTM (American Society for Testing and Materials)

471 and Environmental Protection Agency manual (EPA) strength threshold at 7 days moist curing
472 age (Goodarzi and Movahedrad, 2017).

473

474 **4.2 Linear expansion of stabilised GM soil with MgO-waste binders**

475 The swelling phenomenon in soils is of key interest as it dictates the overall suitability and
476 stability of the soil after stabilisation in preparation for its application for various civil
477 engineering works (subgrades, light building foundations etc). However, the extent of the
478 swelling occurrence is reliant on certain factors such as the particle size distribution, type and
479 amount of mineral present within the soil/clay and any variance in moisture content (Oti et al.,
480 2009a, Oti et al., 2009b). Hafez et al. (2008) and Tran et al. (2014) also reported the deleterious
481 impact of the swelling phenomena as the settlement attributes of the soils when subjected to
482 alternating variations in moisture. Therefore, the variance in the results from the linear
483 expansion tests in the current research, can be used to hypothesize the expected
484 swelling/shrinkage tendencies of GM soil using both calcium based (CEM I) and MgO-waste
485 activated GGBS binders. Hence, a maximum expansion limit of 1.5% as stipulated in the
486 American standard of measurement (ASTM) and a Spanish limit of 3% for stabilised soil
487 systems will be employed as a benchmark in the current investigation (ASTM D4829 - 11,
488 Seco et al., 2011, Diaz Caselles et al., 2020). The magnitude of linear expansion for the control
489 cylinder specimens will also be employed as the secondary benchmark.

490 The stabilised GM soil containing CEM I (Control) demonstrated an astronomical increase in
491 linear expansion as soon as water was introduced into the cylindrical set up after 7-days of
492 moist curing. One significant factor that could have caused the linear expansion could be due
493 to the presence of ettringite crystals which absorbs water upon contact with water (Adeleke et
494 al., 2020, Li et al., 2020). Furthermore, the significant linear expansion exhibited by cylinder
495 specimens that were stabilised with 6 wt.% of 10wt.% MG1:90wt.% GGBS blend composition
496 could be due to the presence of ettringite formation amongst other hydration compounds in the
497 presence of sulphate. This is possible due to the corresponding high amounts of available Ca
498 from increased GGBS content within the blend composition. The reduction in linear expansion
499 that was observed for every increase in the MG1 content within the MG1:GGBS blend
500 compositions at successive stabiliser dosages (6, 8 and 10 wt.%) can be attributed to the
501 increase in the activator content (in this case MgO waste) necessary for improved hydration
502 reaction with the production of more cementitious hydrate compounds. This cementing gel was
503 able to effectively bind and fill up the colloidal spaces within the GM soil particles. In addition,
504 the cementing gel (M-S-H) that was produced coated the available sulphate (gypsum crystals)
505 within the GM soil. This occurrence prevented the gypsum from any further reaction with the
506 available Ca within the hydrating system, that could cause any deleterious impact on the
507 stabilised Gypsum marl soil in the long term. Research works by Jin et al. (2015) and Wang et
508 al. (2016) are in agreement with the earlier hypothesis and suggested that the increased amount
509 of activator (reactive MgO) effectively increases the pH level within a stabilised system, which
510 is essential to activate GGBS for a more active and improved pozzolanic reaction.

511 The significant linear expansion of 9, 1.6 and 1.3% that was observed for Gypsum marl clay
512 cylinder specimens containing 10 wt.% MG1:90 wt.% GGBS (see Figures 6 – 8) seem to
513 reduce with each increasing stabiliser dosage of 6, 8 and 10 wt.%. This could be attributed to
514 the decrease in the activation of the GGBS by the reduced quantity of MG1 within the stabilised
515 system. However, as the stabiliser dosage increased (as seen for blend compositions with 20
516 wt.% and 30wt.% MG1 wastes), there was an increased activity in the hydration reaction to

517 produce more cementing compound (M-S-H gel). Generally, the GM cylinder test specimen
518 with 20 wt.% MG1:80 wt.% GGBS blend composition and 30 wt.% MG1:70 wt.% GGBS
519 blend composition with stabiliser dosages of 6 – 10 wt.% all achieved linear expansion limits
520 within the range of 0.04 – 1.17%, which are well below the established benchmark of 1.5%
521 (ASTM limit), 3% (Spanish limit) and the control cylinder specimen with calcium-based binder
522 (8 wt.% CEM I). This exceptional performance in linear expansion has demonstrated the
523 viability of using MgO-waste activated GGBS binders to stabilise natural soils with high
524 sulphate content.

525

526 **4.3 Microstructural investigation of stabilised GM soil with MgO-waste binders**

527 Microstructural investigation is key to unravelling the mechanism behind the behaviour of
528 stabilised materials by providing visual images of the morphology, and structure of the
529 components of the stabilised cylinder specimen and any cementitious hydrate compound that
530 might have been formed during the hydration reaction (Goldstein et al., 2017). Generally, the
531 flocculated structure observed in the SEM micrographs for the investigated GM test cylinders
532 using both calcium based (Control) and MG1-waste activated GGBS binders after 28 days of
533 moist curing can be attributed to the ion-exchange process, resulting in the replacement of
534 multivalent ions (Ca and Mg) from the activators (CEM I and MG1) with the monovalent
535 cations in the surface of the clay particles (Du et al. (2013) and Goodarzi and Salimi (2015)).

536 The microstructure of both CEM I and MG1:GGBS stabilised GM soil consists of an
537 agglomeration of phases, with a typical morphology of sulphate-bearing minerals such as
538 ettringite and gypsum. Small globular particles clumped together with no definite shape
539 thought to be C-S-H gel and flat sheets of gypsum and ettringite crystal precipitates were
540 visually identified as some of the hydration compounds in the Control cylinder test specimen
541 (Li et al., 2020). Several researchers (Rahmat and Kinuthia, 2011b, Adeleke et al., 2020, Li et
542 al., 2020) have reported that when soils containing some levels of sulphate content react with
543 calcium-based binders (such as PC and lime), which produces Calcium Aluminate Sulphate
544 Hydrate (C-A-S-H) minerals. An example of such mineral is the formation of a needle-like
545 structure known as ettringite, which has a large expansive potential due to its ability to absorb
546 large volumes of water but can remain dormant with no contact with water. Upon partial
547 soaking for 28 days, the ettringite structure caused very high swelling pressure during its
548 formation resulting in a disruptive increase in volume. Furthermore, the ettringite occupied a
549 greater volume than the original constituent reactants (C-S-H gel), which can also have a
550 negative impact on the compressive strength property and binding capacity of the cementing
551 gel (Yi et al., 2015a). However, GM soil that was stabilised with the MG1:GGBS binder
552 indicated no trace of the needle-like ettringite crystal and showed a rather compact structure
553 (flocculated soil articles) composed of the cementitious hydrate (M-S-H gel). This explains the
554 low linear expansion that was observed in Figure 6 - 8 for the GM soil stabilised with
555 MG1:GGBS binders. In addition, the M-S-H gel that was formed during the hydration reaction
556 of MG1-activated-GGBS binder formed a coating around the sheets of gypsum, hereby
557 hindering the expected reaction of any available Ca to react with the gypsum and form ettringite
558 crystals.

559 The presence of voids were more prominently noticed in the micrographs for CEM I stabilised
560 GM soil which indicates a rather weak bonding between the soil particles (Yi et al., 2015a,
561 Gomes and de Oliveira, 2018). However, the presence of voids were almost absent in the case
562 of the MG1:GGBS stabilised GM soil as the soil structure was well integrated with the soil
563 grains and well surrounded by the cementitious hydrate (M-S-H gel). This explains the

564 improved compressive strength of MG1:GGBS stabilised cylinder specimen compared to the
565 CEM I stabilised GM cylinder test specimen (Goodarzi and Movahedrad, 2017). Generally,
566 ettringite was not definite during moist curing, but clearly evident after soaking of the GM
567 cylinders that were stabilised with CEM I.

568

569 CONCLUSION

570 The outcomes from the current study suggest the viability of producing an alternative
571 cementitious binder (MG1:GGBS) by using up to 30 wt.% MgO-waste (MG1) to successfully
572 activate GGBS for stabilising natural soils containing high sulphate content. The following
573 conclusions can be drawn as follows:

- 574 1. The compressive strength of the MG1:GGBS stabilised GM soil was significantly
575 improved above the acceptable limits as set by the ASTM (American Society for
576 Testing and Materials), Environmental Protection Agency manual (EPA) for the use of
577 industrial waste materials using stabiliser dosages within the range of 6 - 10 wt.%. In
578 all mix compositions, the compressive strength resistance was more pronounced using
579 the 10wt.% than for the 6wt.% stabiliser dosage. The UCS of MG1:GGBS stabilised
580 GM soils were 1.5 – 3 times more than the control at the standardised 28 days moist
581 curing age.
582
- 583 2. The MG1:GGBS binder demonstrated resistance to linear expansion as low as 0.13% –
584 0.2% using 30wt.% MG1:70wt.% GGBS mix proportion at all stabiliser dosages (6 -
585 10 wt.%) after 56 days of observation compared with the control blend mix of 3.2%,
586 which is more than the benchmarks as set by the American standard of measurement
587 (ASTM) – 1.5% and Spanish limits – 3% for stabilised soil systems. In addition, the
588 linear expansion reduces with an increase in the stabiliser dosage (6 – 10wt.%) for all
589 mix proportions. However, stabilizer dosage below 6wt.% is not advisable for
590 stabilising high sulphate soils due to the potential for more expansion that is suspected
591 to be caused by ettringite formation.
592
- 593 3. The SEM micrographs for the MG1:GGBS binder stabilised GM soil showed a more
594 compact and dense microstructure compared with the control at 28 day moist cured and
595 soaking conditions. The enhanced microstructure justifies the significant compressive
596 strength increase for the MG1:GGBS stabilised soils. The presence of holes were clearly
597 evident in the SEM micrographs for the control with a morphology of small globular
598 particles clumped together with no definite shape known as C-S-H gel, flat sheets of
599 gypsum and needle-like ettringite prisms after 28 days moist curing. In addition, the
600 flocculated structure produced larger holes when subjected to the partially soaking
601 conditions, which could be due to the increased production of the needle-like ettringite
602 prism upon contact with water and recrystallisation of the gypsum crystals which exerts
603 pressure on the developing cementitious hydrate and causes the stabilised product to
604 disintegrate.
- 605 4. The limitations to this study that could impact on the authenticity of the experimental
606 results are the use of a single soil type with a specific sulphate content (22 wt.%) for
607 the experimentations and the level of technical expertise during the sample preparation.

608

609 **AUTHOR CONTRIBUTIONS**

610 **Adeleke B. O. and Kinuthia J. M. :** Conceptualization, Methodology, Software. **Adeleke B.**
611 **O.:** Data curation, Writing- Original draft preparation. **Adeleke B. O.:** Visualization,
612 Investigation. **Kinuthia J. M. and Oti J. E.:** *Supervision.* **Adeleke B. O., Kinuthia J. M. and**
613 **Oti J. E.:** Software, Validation.: **Kinuthia J. M. and Oti J. E.:** Writing- Reviewing and
614 Editing,

615

616 **CONFLICT OF INTEREST**

617 None

618

619 **REFERENCES**

620 ASTM D4829 - 11. Standard Test Method for Expansion Index of Soils *Annual Book of*
621 *ASTM Standards.* West Conshohocken PA, 2010: ASTM International.

622 BS 1924 - 2:2018. Hydraulically bound and stabilized materials for civil engineering
623 purposes. *Sample preparation and testing of materials during and after treatment.*
624 BSI Standard Limited.

625 BS EN 197-1:2011. Cement. *Part 1: Composition, specifications and conformity criteria for*
626 *common cements.* BSI Standards Limited.

627 BS EN 13286-49:2004. Unbound and hydraulically bound mixtures. *Accelerated swelling test*
628 *for soil treated by lime and/or hydraulic binder.* BSI Standards Limited.

629 BS EN 15167-1:2006. Ground granulated blast furnace slag for use in concrete, mortar and
630 grout —. *Part 1: Definitions, specifications and conformity criteria.* BSI Standards
631 Limited.

632 BS EN 15309:2007. Characterization of waste and soil. *Determination of elemental*
633 *composition by X-ray fluorescence.* BSI Standards Limited.

634 BS ISO 18227:2014. Soil quality. *Determination of elemental composition by X-ray*
635 *fluorescence.* BSI Standards Limited.

636 ABDALQADER, A., F., JIN, F. & AL-TABBAA, A. 2015. Characterisation of reactive
637 magnesia and sodium carbonate-activated fly ash/slag paste blends. *Construction and*
638 *Building Materials*, 93, 506-513, doi: 10.1016/j.conbuildmat.2015.06.015.

639 ADELEKE, B. O., KINUTHIA, J. M. & OTI, J. E. 2020. Strength and Swell Performance of
640 High-Sulphate Kaolinite Clay Soil. *Sustainability*, 12, 10164 - 10168.

641 ARDAH, A., CHEN, Q. & ABU-FARSAKH, M. 2017. Evaluating the performance of very
642 weak subgrade soils treated/stabilized with cementitious materials for sustainable
643 pavements. *Transportation Geotechnics*, 11, 107–119.

- 644 BEHNOOD, A. 2018. Soil and clay stabilization with calcium- and non-calcium-based
645 additives: A state-of-the-art review of challenges, approaches and techniques.
646 *Transportation Geotechnics*, 17, 14-32, doi: 10.1016/j.trgeo.2018.08.002.
- 647 BERNARD, E., LOTHENBACH, B., CHLIQUE, C., WYRZYKOWSKI, M., DAUZÈRES,
648 A., POCHARD, I. & CAU-DIT-COUMES, C. 2019. Characterization of magnesium
649 silicate hydrate (M-S-H). *Cement and Concrete Research*, 116, 309-330, doi:
650 10.1016/j.cemconres.2018.09.007.
- 651 CHENG, K. & HEIDARI, Z. 2018. A new method for quantifying cation exchange capacity
652 in clay minerals. *Applied Clay Science*, 161, 444-455.
- 653 CHESHOMI, A., ESHAGHI, A. & HASSANPOUR, J. 2017. Effect of lime and fly ash on
654 swelling percentage and Atterberg limits of sulfate-bearing clay. *Applied Clay
655 Science*, 135, 190-198, doi: 10.1016/j.clay.2016.09.019.
- 656 DANG, L. C., FATAHI, B. & KHABBAZ, H. 2016. Behaviour of expansive clay stabilized
657 with hydrated lime and Bagasse Fibres. *Procedia Engineering* 143, 658-665.
- 658 DARKO, K. & BRANISLAV, Z. 2002. Effects of dosage and modulus of water glass on
659 early hydration of alkali-slag cements. *Cement and Concrete Research*, 32, 1181-
660 1188.
- 661 DEL VALLE-ZERMEÑO, R., GIRO-PALOMAA, J. & CHIMENOSA, J., M. 2015. Low-
662 grade magnesium oxide by-products for environmental solutions: characterization and
663 geochemical performance. *Journal of Geochemical Exploration*, 152, 134-144.
- 664 DIAZ CASELLES, L., HOT, J., ROOSZ, C. & CYR, M. 2020. Stabilization of soils
665 containing sulfates by using alternative hydraulic binders. *Applied Geochemistry*, 113,
666 doi: 10.1016/j.apgeochem.2019.104494.
- 667 DU, Y. J., JIANG, N. J., LIU, S. Y., JIN, F., SINGH, D. N. & PUPPALA, A. J. 2013.
668 Engineering properties and microstructural characteristics of cement-stabilized zinc
669 contaminated kaolin. *Geotech*, 51, 289 - 302.
- 670 EL-DIEB, A. S. & KANAAN, D. M. 2018. Ceramic waste powder an alternative cement
671 replacement – Characterization and evaluation. *Sustainable Materials and
672 Technologies*, 17, doi: 10.1016/j.susmat.2018.e00063.
- 673 GILIBERTO, E., IOPPOLO, S. & MANUELLA, F. 2008. Ettringite and thaumasite: a
674 chemical route for their removal from cementitious artefacts. *Journal of Cultural
675 Heritage*, 9, 30-37.
- 676 GOLDSTEIN, J. I., NEWBURY, D. E., ECHLIN, P., JOY, D. C., FIORI, C. & LIFSHIN, E.
677 2017. *Scanning Electron Microscopy and X-Ray Microanalysis*, New York, Springer
678 Nature.
- 679 GOMES, C. M. & DE OLIVEIRA, A. D. S. 2018. Chemical phases and microstructural
680 analysis of pastes based on magnesia cement. *Construction and Building Materials*,
681 188, 615-620, doi: 10.1016/j.conbuildmat.2018.08.083.

- 682 GOODARZI, A. & SALIMI, M. 2015. Stabilization treatment of a dispersive clayey soil
683 using granulated blast furnace slag and basic oxygen furnace slag. *Applied Clay*
684 *Science*, 108, 61-69.
- 685 GOODARZI, A. R. & MOVAHEDRAD, M. 2017. Stabilization/solidification of zinc-
686 contaminated kaolin clay using ground granulated blast-furnace slag and different
687 types of activators. *Applied Geochemistry*, 81, 155-165, doi:
688 10.1016/j.apgeochem.2017.04.014.
- 689 GOPINATH, A., BAHURUDEEN, A., APPARI, S. & NANTHAGOPALAN, P. 2018. A
690 circular framework for the valorisation of sugar industry wastes: Review on the
691 industrial symbiosis between sugar, construction and energy industries. *Journal of*
692 *Cleaner Production*, 203, 89-108, doi: 10.1016/j.jclepro.2018.08.252.
- 693 GÓRAK, P., POSTAWA, P., TRUSILEWICZ, L. N. & KALWIK, A. 2020. Cementitious
694 eco-composites and their physicochemical/mechanical properties in Portland cement-
695 based mortars with a lightweight aggregate manufactured by upcycling waste by-
696 products. *Journal of Cleaner Production*, doi: 10.1016/j.jclepro.2020.125156.
- 697 GU, K., JIN, F., AL-TABBAA, A., SHI, B. & LIU, J. 2014. Mechanical and hydration
698 properties of ground granulated blastfurnace slag pastes activated with MgO–CaO
699 mixtures. *Construction and Building Materials*, 69, 101-108, doi:
700 10.1016/j.conbuildmat.2014.07.032.
- 701 HAFEZ, M. A., SIDEK, N. & NOOR, M. J. 2008. Effect of pozzolanic process on the
702 strength of stabilized lime clay. *Electronic Journal of Geotechnical Engineering*, 13.
- 703 JIN, F. & AL-TABBAA, A. 2013. Thermogravimetric study on the hydration of reactive
704 magnesia and silica mixture at room temperature. *Thermochimica Acta*, 566, 162-168,
705 doi: 10.1016/j.tca.2013.05.036.
- 706 JIN, F. & AL-TABBAA, A. 2014. Characterisation of different commercial reactive
707 magnesia. *Advances in Cement Research*, 26, 101-113, doi: 10.1680/adcr.13.00004.
- 708 JIN, F., GU, K. & AL-TABBAA, A. 2015. Strength and hydration properties of reactive
709 MgO-activated ground granulated blastfurnace slag paste. *Cement and Concrete*
710 *Composites*, 57, 8-16.
- 711 JOHN, U. E., JEFFERSON, I., BOARDMAN, D. I., GHATAORA, G. S. & HILLS, C. D.
712 2011. Leaching evaluation of cement stabilisation / solidification treated kaolin clay.
713 *Engineering Geology*, 123, 315-323, doi: 10.1016/j.enggeo.2011.09.004.
- 714 JONES, L. D. & JEFFERSON, I. 2012. Expansive soils. *ICE Manual of geotechnical*
715 *engineering*, 413–41.
- 716 JUENGER, M. C. G. & SIDDIQUE, R. 2015. Recent advances in understanding the role of
717 supplementary cementitious materials in concrete. *Cement and Concrete Research*,
718 78, 71-80, doi: 10.1016/j.cemconres.2015.03.018.
- 719 JUENGER, M. C. G., WINNEFELD, F., PROVIS, J. L. & IDEKER, J. H. 2011. Advances in
720 alternative cementitious binders. *Cement and Concrete Research*, 41, 1232-1243, doi:
721 10.1016/j.cemconres.2010.11.012.

- 722 KINUTHIA, J. M. & OTI, J. E. 2012. Designed non-fired clay mixes for sustainable and low
723 carbon use. *Applied Clay Science*, 59–60, 131–139.
- 724 KINUTHIA, J. M. & WILD, S. 2001. Effects of some metal sulphates on the strength and
725 swelling properties of lime-stabilised kaolinite. *International Journal on Pavement*
726 *Engineering*, 2, 103–120.
- 727 KINUTHIA, J. M., WILD, S. & JONES, G. I. 1999. Effects of monovalent and divalent
728 metal sulphates on consistency and compaction of lime-stabilised kaolinite. *Applied*
729 *clay science*, 14, 27-25.
- 730 LI, W., YI, Y. & PUPPALA, A. J. 2020. Suppressing Ettringite-Induced Swelling of
731 Gypseous Soil by Using Magnesia-Activated Ground Granulated Blast-Furnace Slag.
732 *Journal of Geotechnical and Geoenvironmental Engineering*, 146, doi:
733 10.1061/(asce)gt.1943-5606.0002292.
- 734 LI, Y., SUN, J. & CHEN, B. 2014. Experimental study of magnesia and M/ P ratio
735 influencing properties of magnesium phosphate cement. *Construction and Building*
736 *Materials*, 671, 741-753.
- 737 MIQUELEIZ, L., RAMÍREZ, F., SECO, A., NIDZAM, R., KINUTHIA, J., TAIR, A. &
738 GARCIA, R. 2012. The use of stabilised Spanish clay soil for sustainable construction
739 materials. *Engineering Geology*, 133-134, 9-15.
- 740 NIDZAM, R., M. & KINUTHIA, J., M. 2010. Sustainable soil stabilisation with blastfurnace
741 slag – a review. *Proceedings of the Institution of Civil Engineers - Construction*
742 *Materials*, 163, 157-165.
- 743 NORMAN, R., DANN, S., HOGG, S. & KIRK, C. 2013. Synthesis and structural
744 characterisation of new ettringite and thaumasite type phases:
745 $\text{Ca}_6[\text{Ga}(\text{OH})_6 \cdot 12\text{H}_2\text{O}]_2(\text{SO}_4)_3 \cdot 2\text{H}_2\text{O}$ and $\text{Ca}_6[\text{M}(\text{OH})_6 \cdot 12\text{H}_2\text{O}]_2(\text{SO}_4)_2(\text{CO}_3)_2$, M =
746 Mn, Sn. *Solid State Sciences*, 25, 110-117.
- 747 OLIVIER, J., G., J., & PETERS, J., A., H., W. 2019. Trends In Global CO₂ And Total
748 Greenhouse Gas Emissions. The Hague.
- 749 OLIVIER, J. G. J., JANSSENS-MAENHOUT, G. & PETERS, J. A. H. W. 2012. Trends in
750 Global CO₂ Emissions. *Report; PBL Netherlands Environmental Assessment Agency:*
751 *The Hague, The Netherlands*, 40.
- 752 OTI, J. E., KINUTHIA, J. M. & BAI, J. 2009a. Compressive strength and microstructural
753 analysis of unfired clay masonry bricks. *Engineering Geology*, 109, 230-240, doi:
754 10.1016/j.enggeo.2009.08.010.
- 755 OTI, J. E., KINUTHIA, J. M. & BAI, J. 2009b. Engineering properties of unfired clay
756 masonry bricks. *Engineering Geology*, 107, 130-139, doi:
757 <https://doi.org/10.1016/j.enggeo.2009.05.002>.
- 758 PHANIKUMAR, B. & SINGLA, R. 2016. Swell-consolidation characteristics of fibre-
759 reinforced expansive soils. *Soils and Foundations*, 56, 138-143.

- 760 PRUŠKA, J. & ŠEDIVÝ, M. 2015. Prediction of Soil Swelling Parameters. *Procedia Earth*
761 *and Planetary Science*, 15, 219-224, doi: 10.1016/j.proeps.2015.08.052.
- 762 RAHMAT, M. & KINUTHIA, J. 2011a. Effects of mellowing sulfate-bearing clay soil
763 stabilized with wastepaper sludge ash for road construction. *Engineering Geology*,
764 117, 170-179.
- 765 RAHMAT, M. N. & KINUTHIA, J. M. 2011b. Effects of mellowing sulfate-bearing clay soil
766 stabilized with wastepaper sludge ash for road construction. *Engineering Geology*,
767 117, 170-179, doi: 10.1016/j.enggeo.2010.10.015.
- 768 ROOSZ, C., GRANGEON, S., BLANC, P., MONTOUILLOUT, V., LOTHENBACH, B.,
769 HENOCQ, P., GIFFAUT, E., VIEILLARD, P. & GABOREAU, S. 2015. Crystal
770 structure of magnesium silicate hydrates (M-S-H): The relation with 2:1 Mg-Si
771 phyllosilicates. *Cement and Concrete Research*, 73, 228–237.
- 772 RUAN, S. & UNLUER, C. 2016. Comparative life cycle assessment of reactive MgO and
773 Portland cement production. *Journal of Cleaner Production*, 137, 258–273.
- 774 SCHANZ, T., TRIPATHY, S. & SRIDHARAN, A. 2018. Volume change behaviour of
775 swelling and non-swelling clays upon inundation with water and a low dielectric
776 constant fluid. *Applied Clay Science*, 158, 219-225.
- 777 SECO, A., MIQUELEIZ, L., PRIETO, E., MARCELINO, S., GARCÍA, B. & URMENETA,
778 P. 2017. Sulfate soils stabilization with magnesium-based binders. *Applied Clay*
779 *Science*, 135, 457-464, doi: 10.1016/j.clay.2016.10.033.
- 780 SECO, A., RAMÍREZ, F., MIQUELEIZ, L. & GARCÍA, B. 2011. Stabilization of expansive
781 soils for use in construction. *Applied Clay Science*, 51, 348-352, doi:
782 10.1016/j.clay.2010.12.027.
- 783 SHAND, M. A. 2006. *The Chemistry and Technology of Magnesia*, New York, John Wiley &
784 Sons.
- 785 TRAN, T. D., CUI, Y.-J., TANG, A. M., AUDIGUIER, M. & COJEAN, R. 2014. Effects of
786 lime treatment on the microstructure and hydraulic conductivity of Héricourt clay.
787 *Journal of Rock Mechanics and Geotechnical Engineering*, 6, 399-404, doi:
788 10.1016/j.jrmge.2014.07.001.
- 789 UNITED-NATIONS. 2015. *Transforming our World: The 2030 Agenda for Sustainable*
790 *Development*, [Online]. Available: <https://doi.org/10.1080/02513625.2015.1038080>
791 [Accessed April 2020].
- 792 USGS 2020. Mineral Commodity Summaries. In: INTERIOR, U. S. D. O. T. (ed.). White
793 house - USA: DOI Inspector General.
- 794 WANG, F., JIN, F., SHEN, Z. & AL-TABBAA, A. 2016. Three-year performance of in-situ
795 mass stabilised contaminated site soils using MgO-bearing binders. *J Hazard Mater*,
796 318, 302-307, doi: 10.1016/j.jhazmat.2016.07.018.
- 797 WANG, L., CHEN, L., CHO, D. W., TSANG, D. C. W., YANG, J., HOU, D., BAEK, K.,
798 KUA, H. W. & POON, C. S. 2019. Novel synergy of Si-rich minerals and reactive

- 799 MgO for stabilisation/solidification of contaminated sediment. *J Hazard Mater*, 365,
800 695-706, doi: 10.1016/j.jhazmat.2018.11.067.
- 801 WANG, L., ROY, A., SEALS, R. K. & METCALF, J. B. 2003. Stabilization of Sulfate-
802 Containing Soil by Cementitious Mixtures Mechanical Properties. *Geomaterials*,
803 3724, 12-19.
- 804 WILD, S., KINUTHIA, J., JONES, G. & HIGGINS, D. 1999. Suppression of swelling
805 associated with ettringite formation in lime stabilized sulphate bearing clay soils by
806 partial substitution of lime with ground granulated blastfurnace slag (GGBS).
807 *Engineering Geology*, 51, 257-277.
- 808 WU, H.-L., JIN, F., BO, Y.-L., DU, Y.-J. & ZHENG, J.-X. 2018. Leaching and
809 microstructural properties of lead contaminated kaolin stabilized by GGBS-MgO in
810 semi-dynamic leaching tests. *Construction and Building Materials*, 172, 626-634, doi:
811 10.1016/j.conbuildmat.2018.03.164.
- 812 YI, Y., GU, L. & LIU, S. 2015a. Microstructural and mechanical properties of marine soft
813 clay stabilized by lime-activated ground granulated blastfurnace slag. *Applied Clay
814 Science*, 103, 71-76, doi: 10.1016/j.clay.2014.11.005.
- 815 YI, Y., GU, L., LIU, S. & JIN, F. 2016. Magnesia reactivity on activating efficacy for ground
816 granulated blastfurnace slag for soft clay stabilisation. *Applied Clay Science*, 126, 57-
817 62, doi: 10.1016/j.clay.2016.02.033.
- 818 YI, Y., LISKA, M. & AL-TABBAA, A. 2014. Properties and microstructure of GGBS-MgO
819 pastes. *Advances in Cement Research*, 26, 114-122.
- 820 YI, Y., ZHENG, X., LIU, S. & AL-TABBAA, A. 2015b. Comparison of reactive magnesia-
821 and carbide slag-activated ground granulated blastfurnace slag and Portland cement
822 for stabilisation of a natural soil. *Applied Clay Science*, 111, 21-26, doi:
823 10.1016/j.clay.2015.03.023.
- 824 ZHANG, T., VANDEPERRE, L. J. & CHEESEMAN, C. R. 2014. Formation of magnesium
825 silicate hydrate (M-S-H) cement pastes using sodium hexametaphosphate. *Cement
826 and Concrete Research*, 65, 8-14, doi: 10.1016/j.cemconres.2014.07.001.
- 827
- 828